Inverse problem methodology for thermal-physical properties estimation of frozen green beans

R.C. Martins, C.L.M. Silva *

Escola Superior de Biotecnologia, Universidade Católica Portuguesa, Rua Dr. António Bernardino de Almeida, 4200-072 Porto, Portugal

Keywords: Thermo-physical properties; Inverse problem; Frozen green beans

Abstract

Frozen green beans (*Phaseolus vulgaris*, L.) thermal conductivity (k) and heat capacity (C_p) were determined experimentally by a one dimensional finite difference (transient method) and differential scanning calorimetry, respectively. Thermal properties were also estimated by the inverse problem methodology (IPM). Heat capacity and thermal conductivity behaviour with temperature were modelled by the Schwartzberg equations and linear relationship, respectively below and above the melting point. These equations were used inside a finite element model (FEM) to simulate green beans phase transition under thawing conditions. The sequential simplex method was used to minimise the error vector of the FEM inverse problem, to estimate thermal capacity and thermal conductivity. The accuracy of thermal-physical properties estimated by the two methodologies was compared with data from literature. The thermo-physical properties estimated by the IPM converged for physically meaningful values. Important conclusions were obtained about errors in model predictions. Furthermore, the IPM thermal properties increased the accuracy of simulations, especially during phase transition.

Introduction

One of the most difficult part of frozen foods phase change modelling problems is the characterisation of non-linear thermal properties in time and space, such as, thermal conductivity (k) and thermal capacitance (C_p). Frozen foods do not exhibit a sharp liquid/solid interface that characterises Stefan problems. Foods are multi-component materials that present a phase transition region, where thermal-physical properties can be described by smooth non-linear curves, near the melting point (Voller, 1997).

Heat conductivity (k) and capacitance (C_p) inside the phase transition region depends upon ice crystallisation or melting during freezing and thawing, respectively. Inside this region, thermal-properties can be modelled as functions of temperature.

Linear models have been widely used to describe both heat conductivity and capacitance above the melting point temperature (u_m):

$$C_p = C_{p_m} + \frac{\partial C_p}{\partial u}(u - u_m) \quad (1)$$

$$k = k_m + \frac{\partial k}{\partial u}(u - u_m) \quad (2)$$

where C_{p_m} and k_m are the heat capacitance and conductivity at the melting point temperature (u_m), respectively.

Heat capacity and conductivity determinations are well established at temperatures above the melting point, where no phase change occurs. Heat capacitance is generally determined by adiabatic calorimetry or differential scanning calorimetry (DSC). Thermal conductivity is possible to be determined either by a stationary state method, such as the guarded hot plate, that makes use of the first Fourier law and a heat source in the determination, or by transient methods. Transient methods make use of the second Fourier law for well defined shapes (e.g. infinite slabs, infinite cylinders and spheres) to determine thermal diffusivity (Delgado, Gallo, De Piante, & Rubiolo, 1997).

* Corresponding author. Tel.: +351-22-5580058; fax: +351-22-5090351.

E-mail addresses: r.m.c.m@clix.pt (R.C. Martins), crislui@esb.ucp.pt (C.L.M. Silva).

Nomenclature

a	modified Schwartzberg equation constant, $J\,kg^{-1}\,°C^{-1}$
b	modified Schwartzberg equation constant, $J\,kg^{-1}\,°C^{-2}$
Bi	Biot number
C	capacitance matrix, $J\,K^{-1}$
c	modified Schwartzberg equation constant, $J\,kg^{-1}\,°C$
C_p	heat capacity, $J\,kg^{-1}\,K^{-1}$
d	modified Schwartzberg equation constant, °C
e	fluctuating error vector
f	force vector, W
H	enthalpy, $J\,kg^{-1}$
h	surface heat transfer coefficient, $W\,m^{-2}\,K^{-1}$
IPM	inverse problem methodology
K	stiffness matrix, $W\,K^{-1}$
k	thermal conductivity, $J\,m^{-1}\,K^{-1}$
n	normal to the surface boundary
q^*	heat flux per unit area, $W\,m^{-2}$
t	time, s
u	temperature, °C

Subscripts

∞	refers to environmental condition
0	refers to an initial condition at time zero
app	refers to apparent
f	refers to frozen
m	refers to the melting point
s	refers to the surface

Greek letters

∇	nabla
Ω	physical domain
ρ	density, $kg\,m^{-3}$

Ice melting or crystallisation occurs at discrete locations on the phase transition region. Although phase transition has a discontinuous nature, during thawing or at slow freezing rates, it is macroscopically perceived as a continuous phenomena. Thus, C_p and k have been described by mathematical equations, either empirical or derived using thermodynamic relationships. Lind (1991) presents a vast literature review on the measurement and prediction of frozen foods thermal properties based on thermodynamics.

It is possible to determine the heat capacitance by DSC, as the first derivative of enthalpy in order to temperature: $C_p = \partial H/\partial u$. A theoretical relationship for C_p, as function of composition and temperature, was derived by Schwartzberg (1976). Although the derived relationship gives a good theoretical basis for predicting thermal capacity, Ramaswamy and Tung (1981) found that experimental $C_{p_{app}}$ values increase slightly with temperature when compared with the Schwartzberg equation. Therefore, they included an additional term to the original equation:

$$C_p = a + bu + \frac{c}{(d-u)^2} \tag{3}$$

where a, b, c and d coefficients are obtained by nonlinear regression analysis to the DSC data. This equation generally produces accurate fittings and is suitable for modelling heat capacity inside the phase transition region during freezing at slow freezing rates or thawing.

Thermal conductivity has drastic differentials inside the phase transition region, where k of pure ice is three times greater than liquid water. Many authors developed empirical expressions of thermal conductivity as function of food composition, such as water, ice, protein and fat content (Hermans, 1979; Sweat, 1974). Nevertheless, these expressions do not cope with specific properties of certain foods, such as their shape, fiber and tissue orientations, as well as the direction and position of ice crystals.

Schwartzberg (1981) developed a simple empirical expression to describe thermal conductivity, as function of temperature, below the melting point:

$$k = k_f + (k_m - k_f) \cdot \frac{(u_0 - u_m)}{(u_w - u_m)^2} \tag{4}$$

where k_f and k_m are the thermal conductivities of the frozen and at the melting point, and u_m and u_0 are respectively the temperature of the melting point of green beans and water.

The assumption of continuous thermal-physical properties across the physical domain Ω, enables heat transfer during phase change to be described by a diffusional relationship of temperature, time and space. This partial differential equation is known as the second Fourier law (Ozisik, 1994; Shashkov, 1996):

$$\rho C_p \frac{\partial u}{\partial t} = \nabla(k \nabla u) \tag{5}$$

The solution for this equation depends on the initial an boundary conditions. Typical conditions are for the initial condition:

$$u(\Omega) = u_0 \quad \text{and} \quad t = t_0 \tag{6}$$

where, u_0 is the initial temperature at t_0, the instant zero.

And at the surface boundaries of Ω:

$$k \frac{\partial u}{\partial n} = h \cdot (u_\infty - u_s) \tag{7}$$

where, n is the normal to the surface boundary, h the surface heat transfer coefficient, u_∞ the environmental temperature and u_s the surface temperature.

The finite element method (FEM) approximates the physical domain to a mesh of finite elements, connecting points in space called nodes (Henwood & Bonet, 1996). For each triangular element, a linear relationship between nodes temperatures is used in the solution to the heat transfer problem (Braess, 1997). The final solution to the second Fourier law is reduced to the following linear differential equation (Segerlind, 1984):

$$C\frac{\partial u}{\partial t} + Ku = f \tag{8}$$

where C is the capacitance matrix, expressing the volumetric heat capacitance, K the stiffness matrix, which includes heat conduction and convection effects on nodes temperatures, and f the force vector, that expresses the influence of ambient temperature on nodal temperatures. Nodal temperature evolution can be calculated using a finite difference scheme, such as the Crank–Nicholson.

Generally, frozen foods heat transfer models are assembled using the thermal-physical properties obtained by independent experimental methodologies, such as the ones above referred. Model predictions are thereafter validated against simple shapes, such as infinite slabs and cylinders with well defined analytical solutions of the second Fourier law. Furthermore, prediction are confirmed against freezing or thawing curves, to check model applicability.

This strategy has disadvantages for modelling phase transition, because independent experiments potentially increase the risk of experimental errors propagation to the assembled model, where during phase transition, C_p and k are not independent variables. Thermal-physical properties are much dependent upon the material composition and the process involved (in this case, phase change).

The inverse problem methodology (IPM) tries to overcome the problem of determining dependent physical properties. Instead of using directly the thermal-physical properties obtained experimentally, these are used only as first estimates of an optimisation process. Thus, a mathematical model is optimised against experimental data to obtain its parameters, overcoming the problem of independent measurements of thermophysical properties and their co-variation. This strategy allows to compare model and experimental data for both systematic and random errors, aiding on the identification of unconsidered mechanisms.

This modelling perspective is known as IPM. Therefore, the main objectives of this research were

I. Obtain frozen green beans thermal-physical properties estimates (C_p and k) by conventional experimental methods.
II. Use thermal-physical properties obtained experimentally as first estimates of the IPM optimisation.
III. Investigate the nature of error sources and unconsidered effects on model predictions.
IV. Investigate the applicability of the IPM as a FEM tuning and validation technique.

Materials and methods

Sample preparation

Green beans (*Phaseolus vulgaris*, L.) were obtained from Porto local city market—Portugal, one day after harvesting. They were firstly sorted, washed and blanched in water (2 min at 100 °C). After blanching, green beans were left to cool and dry, and were then frozen in a blast freezer, Armfield FT 36. Samples were frozen at an average air temperature of −40 °C, until the temperature of −35 °C was recorded with a thermocouple placed in the center of a green bean test sample. Approximately 500 g of frozen green beans were immediately put into polyethylene bags (35 cm × 22 cm) and heat-sealed.

Moisture content was determined according to Ehart and Odland (1973), by drying overnight five samples of approximately 5 g of vegetable inside a drying oven (WTB Winder, Germany). The density of the unfrozen sample was measured by Lozano et al. (1980) (cited by Shafiur-Rahman & Driscoll, 1993) technique, using five replications. Green beans density was considered constant in all simulations.

Heat capacity determination

The DSC—heat compensation technique, was used to measure the apparent heat capacity. About 35 mg of green beans were weighted with a microscale (Sartorius micro, Germany) and put into 30 ml aluminium cells (Shimadzu, Japan). The low temperature container LTC 50 (Shimadzu, Japan) was used to decrease temperature until −45 °C, with liquid nitrogen. Thereafter, measurements were carried out in the Shimadzu DSC 50 (Shimadzu, Japan) at a scanning rate of 1 °C/min, in the temperature range of −40 to 30 °C. Five replications were made and an empty cell was used as reference. The obtained thermograms were analysed using the Shimadzu analysis software, with respect to the baseline made with two empty α-alumina cells (Sá, Figueiredo, Correa, & Sereno, 1994).

Thermal condu ctivity estimation

A simple program was developed in MATLAB 4.0 (Pärt-Enander, Sjöberg, Melin, & Isacksson, 1998) to estimate thermal conductivity (k) and surface heat convection coefficient (h).

The thermal conductivity was determined by the transient method using the one dimensional finite difference scheme of the Fourier heat transfer law between the nodal positions 2 and 3, presented in Fig. 1.

Thermocouples were placed at the nodes, and the time–temperature spectrum was recorded. The distance between nodes was measured with a calliper after the thermocouples removal. The thermal capacity (C_p), previously obtained by the DSC method, was used as a known variable to enable the estimation of the thermal conductivity. A thermocouple was placed in the air (thermocouple no. 3, Fig. 1), near the surface, to try to estimate the surface heat transfer coefficient (h). Two replications of a thawing curve were performed using the same green bean specimen, as described in Section 2.1.

The structure in Fig. 1 was built to control the thawing experiment. A green bean sample is placed inside an expanded polyethylene, to increase thermal insulation and expose only one surface to the air. This sets the heat flow to minimal during thawing, making up a controllable experiment, that allows thawing curves replicates to be obtained with low variations in the time–temperature spectrum. Furthermore, a small headspace is left to maintain a stagnated air layer (see Fig. 1), so that the convection coefficient h is controllable to some extent. The stagnated air maintains low Biot numbers (0.05–0.11) (see Fig. 1).

Under low Biot numbers, values of 10–14 $W\,m^{-2}\,K^{-1}$ for the heat convection coefficient are generally obtained. These values were confirmed during the experiment for thermal conductivity estimation. Thus, the average surface convection coefficient value of 12 $W\,m^{-2}\,K^{-1}$ was considered as a fixed value during the following analysis.

Regression analysis for thermal-physical properties estimation

Regression analysis for model fitting was also performed using all replicates data in Section 2.3, by maximising the likelihood function to the thermal conductivity and capacitance equations (2)–(4) and (3)–(1), to estimate their coefficients above and below freezing, respectively. A computer program was developed with the C++ language, using the BLITZ++ Library C++ code (Veldhuizen, 1999), and the Gauss–Newton optimisation algorithm to solve the normal equations and determine the parameter estimates. The estimated parameters variance was obtained by the variance–covariance matrix of the regression coefficients and the model standard deviation was estimated by the mean standard error (Bates & Watts, 1988; Neter, Kutner, Nachtsheine, & Wasserman, 1996). The studentised effect $(\beta_i/s\{\beta_i\})$ of each parameter was computed to define its statistical importance at a 5% confidence level (double sided T-test). The semi-studentised residuals were examined for outlayers, randomness and tested for normality to assess the quality of the fitted kinetic models. Fittings validity was also evaluated by the lack of fit test (Box, Hunter, & Hunter, 1978).

Inverse problem methodology

Heat conduction law is generally considered deterministic. Nevertheless, uncertainties arise from systematic or random errors do affect the Fourier laws and the

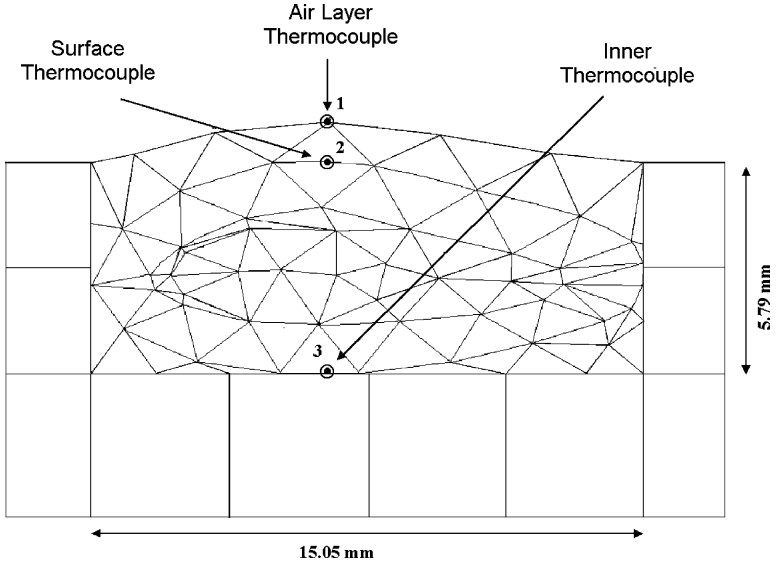

Fig. 1. Mesh used in the inverse problem methodology: (1) air temperature thermocouple, (2) surface thermocouple and (3) inner thermocouple.

thermal-physical parameters. The uncertainty sources are possible to be examined by including a stochastic term into the heat conduction law:

$$q^* = k\nabla u + e(\Omega, t) \tag{9}$$

where q^* is the heat flux per unit area and $e(\Omega, t)$ is a random stochastic function across the physical domain Ω.

This simple modification gives a stochastic interpretation to phase change. Such modification states that energy flow during phase change generally follows the deterministic fourier law, but, at discrete positions of Ω, it is subjected to unknown perturbations. Unknown perturbations can arise from many multiple sources, and for the sake of simplicity of a first approach are considered as independent. During freezing or thawing unconsidered effects, such as nucleation and crystal growth and melting kinetics, are possible sources of systematic errors on thermal-physical properties. Furthermore, uncertainties on the tissue matrix composition and structure present very significant effects during freezing and thawing heat transfer problem. Thus, the second Fourier law, that describes transient heat transfer with and independent stochastic source function, is presented:

$$\rho C_p \frac{\partial u}{\partial t} = \nabla(k\nabla u) + \nabla e(\Omega, t) \tag{10}$$

which can be expressed in the linear form:

$$C\frac{\partial u}{\partial t} + Ku - f = e \tag{11}$$

where e is the fluctuating error vector.

This stochastic finite element equation (SFEM) preserves the Fourier heat transfer equations, but temperature and heat flow are subjected to unknown local perturbations. If errors are random and no tendencies are observed, the heat transfer model is using the most important effects, and variability is attributed to independent sources, to which their expected value is zero.

Under these circumstances, one can consider that the freezing or thawing curves are well described by the Fourier law, and the phase change problem is described by a non-linear diffusional equation. Thus, C_p and k can be determined simultaneously by minimising the error vector (e). Error minimisation is achieved by changing the constants of equations (1)–(4), that describe phase change non-linearity.

Multivariable optimisation is achievable by several optimisation methods. Nevertheless, evolutionary optimisation methods have proven to be very effective on complex optimisations, such as the one performed. The sequential simplex optimisation method has proven to be very efficient in finding the optimum region (Walters, Morgan, Parker, & Deming, 1999), and was used to estimate parameters in Eqs. (1)–(4). Constrains were applied to obtain physical meaningful estimates. Table 1 presents the constrain intervals for thermal-physical properties. The model was optimised against the temperature of two thawing curves at points (2) and (3) of Fig. 1. The meshing of this figure was obtained using the Delaunay triangulation algorithm on a green beans scanned image.

The simplex optimisation was set not to change the surface heat transfer coefficient. Good estimations of the surface heat transfer coefficient (h) are possible with a large number of thermocouples placed inside and on the green beans surface. For such small specimen, it is difficult to map correctly the thermocouples, and the increase in thermocouple number changes significantly the physical domain, and consequently the proposed finite element model. Moreover, the simultaneous optimisation of all three thermal-physical properties h, C_p and k increases the difficulty in the simplex optimisation convergence to physically meaningful values.

The thawing curve was preferred to perform the IPM, in order to increase reproducibility. By thawing at environmental conditions, it is possible to maintain surface heat coefficient at low and constant values, and obtain better results than when using a freezing curve. Although the environmental temperature is not controllable, this factor is accounted also for IPM. Frozen green beans were thawed from an initial temperature of −15 °C, at the room temperature of +20 °C.

It must be emphasised that frozen foods thermal-physical properties, such as C_p and k obtained by

Table 1
Thermal-physical constrains for sequential simplex optimisation

Thermal-physical property	Unfrozen	Frozen
Thermal conductivity ($W\,m^{-1}\,K^{-1}$)	0.3–0.8	0.7–1.8
Apparent heat capacity ($J\,kg^{-1}\,K^{-1}$)	3.2–4.1	1.5–2.3
Surface heat transfer ($W\,m^{-1}\,K^{-1}$)	9–15	
Moisture[a] (%)	90.76	
Density[a] ($kg\,m^{-3}$)	1200	
Freezing point (°C)	−0.221	
Maximum heat of fusion[b] ($kJ\,kg^{-1}$)	282–302	
Maximum enthalpy difference between −15 and −0.22 °C ($kJ\,kg^{-1}$)	311–332	

[a] Average from five replications.
[b] Moisture (%) × 333.2 × 10^{-2} $kJ\,kg^{-1}$.

thawing experiments, are possible to be used in freezing simulations, when supercooling is negligible.

Results and discussion

Apparent heat capacity determination

Green beans initial freezing point was detected in the DSC thermogram heat peak at −0.221 °C. Thermograms were converted into the enthalpy difference vs. temperature curve presented in Fig. 2.

The enthalpy difference obtained by DSC between −15 and 0 °C has the value of 279.88 kJ kg^{-1}. This value is below the expected when one takes into account the water content of green beans (in accordance to Weast & Astle, 1981), as presented in Tables 2 and 3. Nevertheless, data reported in literature agrees with the obtained enthalpy difference. For example, for the same temperature range, enthalpy differences of 283, 244, and 165 kJ kg^{-1} were obtained for apple, pear and tomato, respectively (Sá et al., 1994).

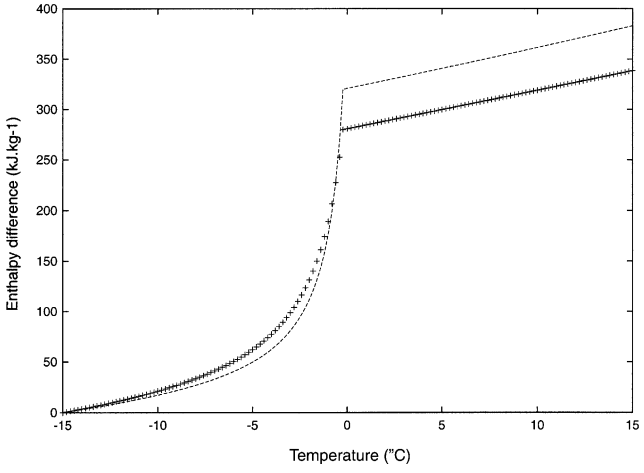

Fig. 2. Green beans enthalpy estimation by DSC (+) and inverse problem methodology (−).

Above the freezing point, heat capacity is within the expected limits, and follows a linear increase with temperature, from 3.765 to 3.892 kJ kg^{-1} in the range of 0–10 °C.

The apparent heat capacity regression parameter estimates to the modified Schwartzberg equation (Eq. (3)) and linear model, respectively below and above the melting point u_m, are presented in Table 2, and shown in Fig. 3. Both models exhibit a good correlation coefficients, between fitted and experimental data, 0.9997 and 0.9983, respectively. Thus, both passed the lack of fit test ($p > 0.05$), and parameters studentised effect is significant ($t(\beta_i) > t(1-\alpha/2; df)$). The estimated models agree with published data by Sá et al. (1994). Therefore, are suited as first apparent heat capacity estimate to be used in the IPM.

Thermal conductivity estimation

Thermal conductivity regression estimates are presented in Table 2. Fittings to experimental data are shown in Fig. 4. Both Schwartzberg equation (Eq. (4)) and linear model (Eq. (2)) exhibit a good correlation coefficient between model and experimental data, 0.8834 and 0.8964, respectively. The parameters studentised effect is also significant (see Table 2).

The finite difference scheme is capable of giving good thermal conductivity estimates with temperature. Nevertheless, k estimates are very sensitive near the melting point u_m. This effect has already been verified, with the transient probe methodology, by Wang and Kolbe (1990). During the initialisation of phase change, the large amount of latent heat makes temperature to remain almost constant. Therefore, as temperature differences between nodes are very small, the calculated thermal conductivity is very sensitive to fluctuations in the temperature record.

Table 2
Green beans unfrozen apparent heat capacity ($C_{p_{app}}$), unfrozen and frozen thermal conductivity (k) equation parameters, estimated by regression and sequential simplex optimisation

$u > u_m$	C_{p_m} (kJ kg^{-1} K^{-1})	$\partial C_p/\partial u$ (kJ kg^{-1} K^{-2})	SE
C_p[a]	$3.783 \pm 3.313 \times 10^{-2}$	$1.067 \times 10^{-2} \pm 2.323 \times 10^{-3}$	0.433
C_p[b]	$3.883 \pm 3.523 \times 10^{-2}$	$1.080 \times 10^{-2} \pm 3.081 \times 10^{-3}$	–
$u > u_m$	k_m (W m^{-1} K^{-1})	$\partial k/\partial u$ (W m^{-1} K^{-2})	
k[a]	0.624 ± 0.000	$1.060 \times 10^{-2} \pm 3.772 \times 10^{-4}$	1.786×10^{-2}
k[b]	0.624 ± 0.001	$0.306 \times 10^{-2} \pm 0.119 \times 10^{-3}$	–
$u < u_m$	k_m (W m^{-1} K^{-1})	k_f (W m^{-1} K^{-1})	
k[a]	0.624 ± 0.004	1.407 ± 0.005	0.072
k[b]	0.624 ± 0.022	1.389 ± 0.032	–

[a] Non-linear regression estimation.
[b] IPMP—sequential simplex optimisation.

Table 3
Green beans frozen apparent heat capacity ($C_{P_{app}}$), estimated by regression and sequential simplex optimisation

$u < u_m$	a (kJ kg^{-1} °C^{-1})	b (kJ kg^{-1} °C^{-2})	c (J kg^{-1} °C)	d (°C)	SE
C_p[a]	1.822 $\pm 5.952\times10^{-2}$	8.231 $\pm 1.785\times10^{-3}$	474.3 ± 4.441	1.553 $\pm 1.027\times10^{-2}$	0.650
C_p[b]	1.812 $\pm 2.193\times10^{-2}$	7.675 $\pm 0.181\times10^{-3}$	290.2 ± 18.535	0.801 $\pm 8.476\times10^{-2}$	–

[a] Non-linear regression estimation.
[b] IPM—sequential simplex optimisation.

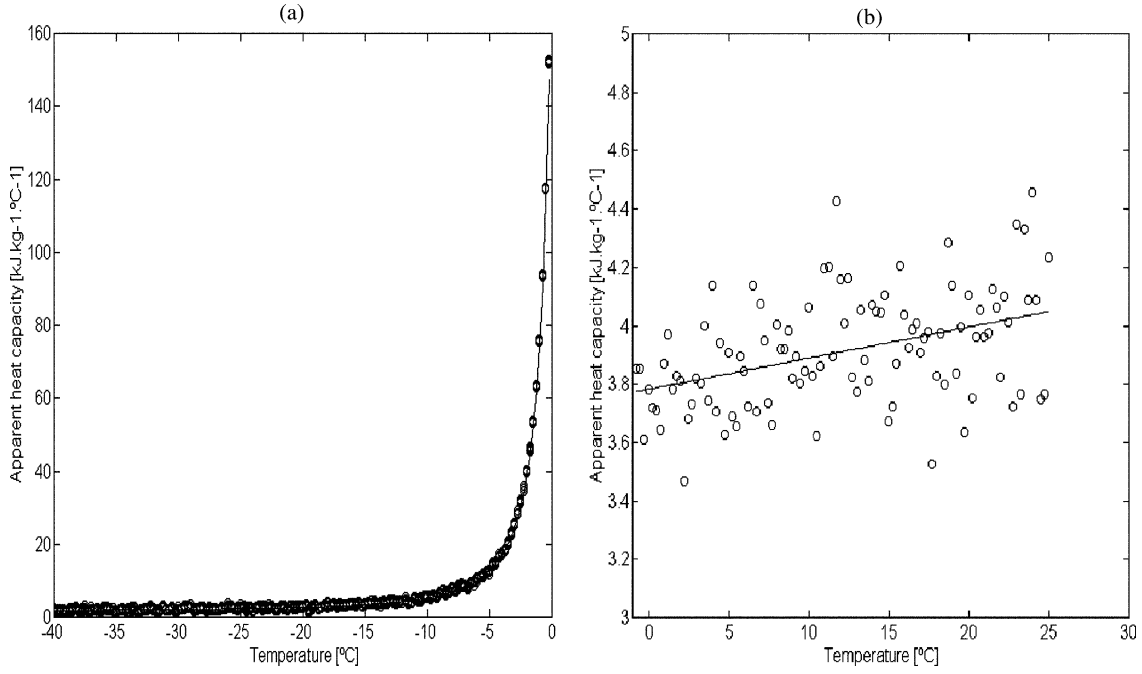

Fig. 3. Heat capacity regression analysis: (a) heat capacity below the melting point and (b) heat capacity above the melting point.

Furthermore, this method is very sensitive to errors in the thermocouples distance, because green beans are not very wide (5.79 mm approximately; see Fig. 1). Thus, special care has to be taken while measuring thermocouples distances. A good methodology is to make an axial cut between the two holes made by thermocouples punctures. Thereafter, it is possible to make a scanned computer image and estimate the exact thermocouple location by image analysis.

Thermal conductivity data is limited. Available results are within the ranges of 0.4–0.9 and 0.9–1.8 W m^{-1} K^{-1}, for unfrozen and frozen foods, respectively. The wide range is attributed to several reasons, such as sample variety and variability, water content, tissue composition and orientation to the heat source and determination methodology (Delgado et al., 1997; Sweat, 1974; Wang & Hayakama, 1993). Thus, a direct comparison between results is not possible to be performed. However, it is possible to state that obtained thermal conductivity model estimates are within the published ranges for frozen and unfrozen foods, and therefore can be used as first estimates in the IPM.

Inverse problem analysis

Thermal capacity and conductivity IPM estimates are presented in Tables 2 and 3. Fig. 5 presents the optimised thawing curve by the inverse methodology and its studentised residuals. During the realisation of this thawing curve, no vapour condensation was observed on green beans surface.

The sequential simplex converged very rapidly in regions (I) and (III) of Fig. 5a. Lower conversion rates were obtained in region (II). The algorithm converged satisfactory, fitting between the FEM model and the experimental data. The model standard error (SE) of ±1.15 °C, and its correlation coefficient of 0.98, obtained between model prediction and experimental data are very satisfactory. Thus, the model passed the statistical lack of fit test ($p > 0.05$). However, Fig. 5b exhibits a time correlation of studentised residuals, indicating that the FEM model has both systematic and random inaccuracies.

Inside region (I) of Fig. 5a, thermal conductivity presents a small decrease as temperature raises to the

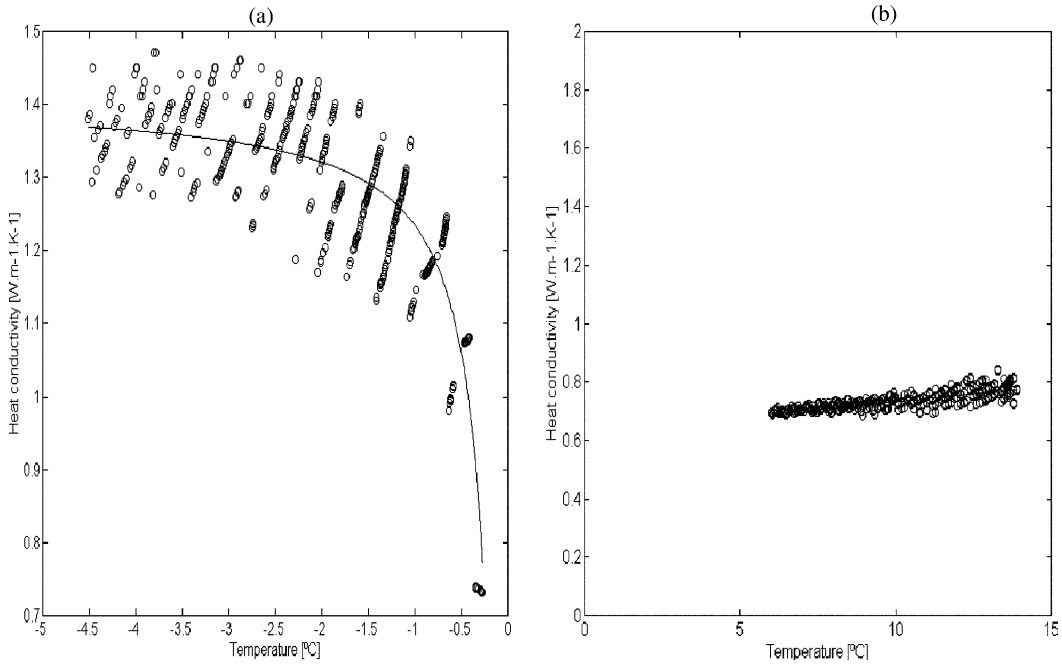

Fig. 4. Thermal conductivity regression analysis: (a) thermal conductivity below the melting point and (b) thermal conductivity above the melting point.

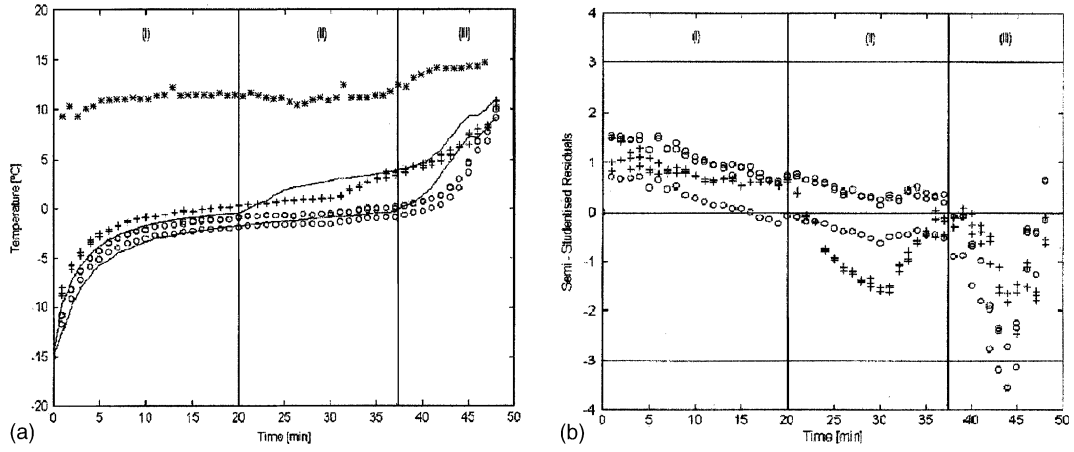

Fig. 5. Green beans simulated thawing curve vs. raw data: (–) FEM model prediction for temperatures in thermocouples 3 and 2, (+) surface thermocouple, (○) inner thermocouple, and (∗) air temperature.

melting point u_m. Thermal capacity (C_p) remains in the region of linear increase with temperature ($u < -10$ °C). It is possible to observe that at low temperatures (<−10 °C in Fig. 2), the enthalpy difference obtained by IPM optimisation is very similar to the obtained by DSC analysis. Thus, at low temperatures both IPM and experimental determinations of C_p and k are in agreement.

However, semi-studentised residuals present a linear decrease in zone (I) (see Fig. 5b). The lack of accuracy in the initial temperature and temperature distribution inside green beans, poor control of room temperature, the influence of the thermocouples and a small sub-estimation of the surface heat transfer coefficient in this region of the thawing curve, are possible sources of this small offset.

Phase change dominates zone (II) in Fig. 5a. Model residuals decrease with a linear trend until their minimum value, near the melting point temperature (u_m) (see Fig. 5b). During this temperature interval, both C_p and k change abruptly, and therefore, most of the optimisation effort of the simplex was spent in this region.

The simulated thawing curve, using the experimental estimates of C_p and k, estimated a thawing time of 40 min. This underestimation is mainly attributed to a sub-estimation of the enthalpy content of frozen green beans between −10 and −0.221 °C. Fig. 2 presents frozen green

beans enthalpy difference obtained by DSC and IPM, where at the melting temperature u_m the enthalpy peak is 279.88 and 320.30 kJ kg^{-1}, respectively. The optimised peak is near the expected range of enthalpy difference for the high water content of green beans and calculated by Weast and Astle (1981) formula (see Table 1). Thus, it is observed experimentally that the DSC underestimates the enthalpy difference by 10.14%, when compared to the IPM optimisation.

It is also observable, in Fig. 2, that the optimised curve is steeper, which is a consequence of green beans high moisture content. The modified Schwartzberg equation parameters (Eq. (3)) that control this region of the enthalpy curve are c and d. Table 3 presents that c decreased from 474.3 to 290.3 J kg^{-1} K, and d decreased from 1.553 to 0.801 °C, respectively.

It is also possible to observe that the optimised IPM FEM model is capable to describe the behaviour of the surface temperature (see Fig. 5). The sigmoidal behaviour at the surface, especially in phase II, is a consequence of the complete defrost of these cell layers. A small offset is observed in the predictions of the surface temperature. Uncertainties on the thermocouple location, convection heat transfer coefficient and in the thickness of the limit air layer may be behind this systematic error.

Errors in phase (III) have a slight increase, where three outlayers exist. The thermocouple no. 3 (Fig. 5) increases its temperature much more rapidly until 10 °C. Nevertheless, the final thawing time is reasonably the same, and residuals show an abrupt tendency towards zero. One probable cause of this deviation is the assumption of a constant value for the surface heat convection coefficient (h), which may over-estimates the heat transfer ratio.

Above the freezing point there are no significant differences in the estimated heat capacity between model optimisation and DSC results.

Small differences were detected in thermal conductivity at the freezing point (k_u). The simplex optimisation shows that thermal conductivity is 66% less sensitive to the temperature increase than the expected from the finite differences method.

Conclusions

The IPM is capable to estimate the apparent heat capacity and thermal conductivity of frozen green beans during thawing. Heat capacity values determined by DSC agreed with published data. However, the DSC underestimated phase change enthalpy, and consequently thawing time.

IPM has a great potential to deal with the non-linearity of the frozen green beans phase change problem. The high variability of the fruits and vegetables thermal properties, makes difficult to compare the obtained values with the expected range. IPM has shown to help to trace and correct the uncertainties to some extent, giving information on model faults, aiding the researcher to build better and more complex models to simulate phase transition, rather than just fitting models to experimental data.

Acknowledgements

The author R.C. Martins gratefully acknowledges his PhD grant (PRAXIS XXI BD/18541/98) to the Fundação para a Ciência e Tecnologia (FCT), Portugal.

References

Bates, D., & Watts, D. (1988). *Non-linear regression analysis and it's applications*. New York: John Wiley & Sons.

Box, G., Hunter, W., & Hunter, J. (1978). *Statistics for experimenters*. New York: Wiley.

Braess, D. (1997). *Finite elements. Theory, fast solvers, and applications in solid mechanics*. Cambridge: Cambridge University Press.

Delgado, A., Gallo, A., De Piante, D., & Rubiolo, A. (1997). Thermal conductivity of unfrozen and frozen strawberry and spinach. *Journal of Food Engineering, 31*, 137–146.

Ehart, M., & Odland, D. (1973). Quality of frozen green vegetables blanched in four concentrations of ammonium bicarbonate. *Journal of Food Science, 38*, 954–958.

Henwood, D., & Bonet, J. (1996). *Finite elements, a gentle introduction*. London: Macmillan Press.

Hermans, F. (1979). The Thermal Diffusivity of Foods. PhD Thesis, The University of Leuven, Netherlands.

Lind, I. (1991). The measurement and prediction of thermal properties of food during freezing and thawing, a review with particular reference to meat and dough. *Journal of Food Engineering, 13*, 285–319.

Neter, J., Kutner, M., Nachtsheine, C., & Wasserman, W. (1996). *Applied linear statistical models* (4th ed.). Chicago: IRWIN.

Ozisik, M. (1994). *Finite differences in heat transfer*. London: CRC Press.

Pärt-Enander, E., Sjöberg, A., Melin, B., & Isacksson, P. (1998). *The MATLAB handbook*. Hallow, England: Addison-Wesley.

Ramaswamy, H. S., & Tung, M. A. (1981). Thermo-physical properties of apples in relation to freezing. *Journal of Food Science, 46*, 724–728.

Sá, M., Figueiredo, A., Correa, A., & Sereno, A. (1994). Apparent heat capacities, initial melting points and heats of melting of frozen fruits measured by differential scanning colorimetry. *Revista Española de Ciencia y Tecnologia de Alimentos, 34*, 202–209.

Schwartzberg, H. G. (1976). Effective heat capacities for freezing and thawing of food. *Journal of Food Science, 41*, 153.

Schwartzberg, H. G. (1981). Mathematical analysis of the freezing and thawing of foods, in Tutorial presented AIchE Summer Meeting, Detroit, Michigan.

Segerlind, L. (1984). *Applied finite element analysis* (2nd ed.). New York: Macmillan Press.

Shafiur-Rahman, M., & Driscoll, R. (1993). Density of fresh and frozen seafood. *Journal of Food Science, 17*, 121–140.

Shashkov, M. (1996). *Conservative finite-difference methods on general grids*. London: CRC Press.

Sweat, V. (1974). Experimental values of thermal conductivity of selected fruits and vegetables. *Journal of Food Science, 39*, 1080.

Veldhuizen, T. (1999). 'Blitz++ user's guide', URL http://oonumerics.org/blitz/BLITZ++.ps.

Voller, V. (1997). An overview of numerical methods for solving phase change problems. In W. Minkowycz & E. Sparrow (Eds.), *Advances in numerical heat transfer* (vol. I, pp. 341–380). London: Taylor & Francis.

Walters, F., Morgan, S., Parker, L., & Deming, S. (1999). *Sequential simplex optimisation*. Boca Raton: CRC Press.

Wang, D., & Kolbe, E. (1990). Thermal conductivity of surimi—measurement and modelling. *Journal of Food Science, 55*, 1217–1221.

Wang, J., & Hayakama, K. (1993). Thermal conductivities of starch gels at high temperatures influenced by moisture. *Journal of Food Science, 58*, 884–887.

Weast, R. C., & Astle, M. J. (1981). *Handbook of chemistry and physics*. Boca Raton: CRC Press.